American Mineralogist, Volume 93, pages 63–73, 2008

Metamorphic vanadian-chromian silicate mineralization in carbon-rich amphibole schists from the Malé Karpaty Mountains, Western Carpathians, Slovakia

Pavel Uher,[1,*] Martin Kováčik,[2] Michal Kubiš,[3] Alexander Shtukenberg,[4] and Daniel Ozdín[5]

[1]Department of Mineral Deposits, Comenius University, Mlynská dolina, 842 15 Bratislava, Slovakia
[2]Geological Survey of the Slovak Republic, Mlynská dolina 1, 817 04 Bratislava, Slovakia
[3]Geofos, s.r.o., Veľký Diel 3323, 010 08 Žilina, Slovakia
[4]Crystallography Department, St. Petersburg State University, Universitetskaya nab., 7/9, 199034, St. Petersburg, Russia
[5]Department of Mineralogy and Petrology, Comenius University, Mlynská dolina, 842 15 Bratislava, Slovakia

Abstract

Mineralization, involving vanadian-chromian silicates, has been studied in Lower Paleozoic, carbon-rich amphibole schists with pyrite and pyrrhotite near Pezinok, southwest Slovakia. A detailed electron microprobe study has revealed the presence of V,Cr-rich garnet, clinozoisite, and muscovite, associated with amphiboles (magnesiohornblende, tremolite, actinolite, and edenite), diopside, and albite. The garnet contains 5–19 wt% V_2O_3, 5–11 wt% Cr_2O_3, and 2–13 wt% Al_2O_3 (16–64 mol% goldmanite, 19–36 mol% uvarovite, and 9–59 mol% grossular end-members). The garnet is unzoned or shows V-rich cores and Al-rich rims, or irregular coarse oscillatory zoning with V, Cr, and Al, locally involving Ca and Mn as well. The V,Cr-rich clinozoisite to mukhinite and "chromian clinozoisite" contains 2–9.5 wt% V_2O_3 and 1.5–11 wt% Cr_2O_3; the muscovite contains 2.5–8 wt% V_2O_3 and 0–7 wt% Cr_2O_3. The mineralization originated from primarily V-, Cr-, and C-rich mafic pyroclastic rocks, affected by volcano-exhalative processes. These rocks were weakly metamorphosed during early Hercynian regional metamorphism (M1), followed by late-Hercynian contact metamorphism (M2) with crystallization of V,Cr-rich silicates, diopside, amphiboles, phlogopite, titanite, albite, quartz, carbonate, pyrite, and pyrrhotite. The youngest Alpine(?) retrograde metamorphic event (M3) is connected with production of V,Cr-poor muscovite, clinochlore, clinozoisite, pumpellyite-(Mg), prehnite, quartz, and carbonates, under prehnite-pumpellite facies conditions.

Keywords: V and Cr mineralization, amphibole schists, contact metamorphism, goldmanite, uvarovite, mukhinite, Western Carpathians, Slovakia

Introduction

Vanadium-rich silicate phases are found in mineral associations from metamorphosed fine-grained pyroclastic and clastic sediments rich in organic carbonaceous matter or from skarns, calcareous metapelites and marbles, associated with mafic rocks. Vanadian grossular to goldmanite [$Ca_3V_2(SiO_4)_3$], a V-dominant member of the ugrandite garnet subgroup, is the most conspicuous mineral in such associations, together with other V-rich phases including micas, diopside, amphiboles, titanite, biotite, oxide minerals, and even sillimanite (e.g., Moench and Meyrowitz 1964; Karev 1974; Suwa et al. 1979; Benkerrou and Fonteilles 1989; Canet et al. 2003; Donohue and Essene 2005). Moreover, goldmanite has been described in refractory inclusions from the Leoville carbonaceous chondrite (Simon and Grossman 1992). Vanadian clinozoisite to mukhinite [$Ca_2Al_2V^{3+}(Si_2O_7)(SiO_4)O(OH)$], in association with goldmanite, has been described in marbles from the Tashegilskoye deposit, Siberia, Russia (Shepel and Karpenko 1969). Vanadian epidote to allanite occurs in association with goldmanite, vanadoan muscovite, vanadoan titanite, and tomichite in the main ore zone of the Hemlo gold deposit, Ontario, Canada (Pan and Fleet 1991, 1992).

The above-mentioned minerals are V-rich but relatively Cr-poor in most localities. However, in the Poblet area, Spain, V- and Cr-rich goldmanite and other minerals have been described (Canet et al. 2003). Donohue and Essene (2005) have also described chromian hercynite with vanadoan sillimanite. Our investigated occurrences in the Pezinok-Pernek crystalline complex, Malé Karpaty Mountains, Slovakia, represent another example of a rare V- and Cr-rich metamorphic association containing garnet (goldmanite-uvarovite-grossular s.s.) with other V- and Cr-rich silicate minerals. Preliminary results were reported by Uher et al. (1994). New mineralogical and petrogenetic results, based on detailed electron-microprobe analysis (EMPA) and X-ray diffraction (XRD) data, are the subject of this contribution.

* E-mail: puher@fns.uniba.sk

Regional geology

The Pezinok-Pernek crystalline complex (PPCC) is a part of the pre-Alpine basement of the Central Western Carpathians. The PPCC represents volcano-sedimentary sequences of Lower Paleozoic metamorphic rocks, mainly metapelites to metapsammites, metabasaltic rocks, black schists, rarely quartzites, all of which have been intruded by Hercynian orogenic granitic plutons (Cambel 1958; Buday et al. 1962; Cambel and Khun 1983), ca. 20 km NE of Bratislava in SW Slovakia (Fig. 1). The PPCC is situated in the Malé Karpaty Mountains, the westernmost situated horst structure of the Tatric Superunit, a link between the Western Carpathians and the Eastern Alps (Maheľ 1986).

Palynological study indicates a Silurian to Devonian age for the PPCC volcano-sedimentary sequences (Cambel and Planderová 1985). The geological structure of the PPCC was formed during the Hercynian (Devonian to Carboniferous) orogeny and represents remnants of a suture zone after obduction and syn-collisional exhumation of oceanic crust represented by the Pernek Group on the metamorphosed, passive continental margin of the Pezinok Group (Ivan et al. 2001; Putiš et al. 2004).

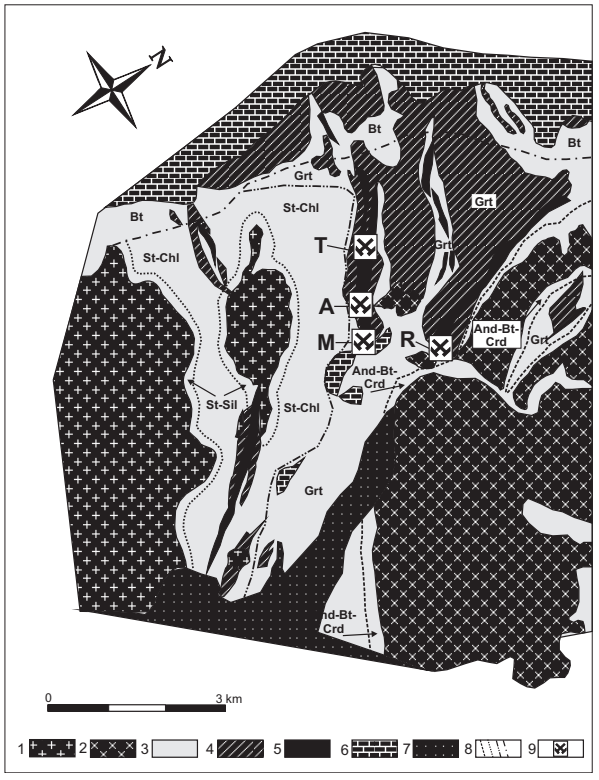

Figure 1. Geological map of the Pezinok-Pernek crystalline complex (PPCC) with sample locations (adapted from Korikovsky et al. 1984 and Uher et al. 1994). Explanation: 1 = Bratislava granitic massif, 2 = Modra granitic massif, 3 = metapelites and metapsammites, 4 = metabasic rocks, 5 = carbon and pyrite/pyrrhotite-rich mafic metapyroclastic rocks ("productive zones"), 6 = Mesozoic clastic and carbonate sediments, 7 = Cenozoic clastic rocks, 8 = metamorphic isograds, 9 = abandoned adits. Mineral abbreviations: And = andalusite, Bt = biotite, Chl = chlorite, Crd = cordierite, Grt = garnet, Sil = sillimanite, St = staurolite. Locality abbreviations: A = Lower Augustín and Upper Augustín, M = Michal, R = Rybníček, T = Trojárová.

Paleozoic basement rocks of the PPCC were tectonically juxtaposed as synmetamorphic (pre-granitic) nappes (Putiš et al. 2004). The volcano-sedimentary rocks of the PPCC were regionally metamorphosed presumably during the Late Devonian (380 ± 20 Ma, whole-rock Rb-Sr isochron age; Bagdasaryan et al. 1983; Cambel et al. 1990) under lower to middle greenschist-facies conditions (Korikovsky et al. 1984). The Modra I-type tonalites, granodiorites, and rarely granites of Carboniferous age (324 ± 10 Ma, Bagdasaryan et al. 1982; 345 ± 22 Ma, Finger et al. 2003) were emplaced into the PPCC volcano-sedimentary sequences with a distinct contact-metamorphic thermal overprint that reached cordierite-andalusite (Korikovsky et al. 1985; Fig. 1). The maximum *P-T* conditions of the metamorphic aureole around the Modra granitic massif can be approximately 560–580 °C and 1.5–2 kbar (Korikovsky et al. 1985; Cambel et al. 1989).

The Alpine (Cretaceous) orogeny caused a very low grade metamorphic overprint during cataclasis of the basement-cover rocks that were thrust over the Mesozoic units to the NW (Putiš 1987; Plašienka et al. 1993). Neo-Alpine (Miocene to Quaternary) uplift has exhumed the Paleozoic basement to the present level.

Occurrences of metamorphic V-Cr mineralization in the PPCC are connected with metamorphosed C-rich amphibole schists, commonly associated with pyrite-pyrrhotite stratiform (SEDEX-type) ore horizons (so-called "productive zones," Cambel 1958). These metamorphosed schists with the ore horizons form intercalations (tens of meters thick), which primarily represent pyroclastic material with an important organic matter admixture. They were incorporated into huge basalt lava flows, which have been metamorphosed into massive amphibolites.

Analytical methods

The chemical compositions of the V-Cr silicate minerals were determined using a JEOL JXA 733 Superprobe and a CAMECA SX100 electron microprobe in wavelength dispersive mode at the Geological Survey of the Slovak Republic, Bratislava. Operating conditions were set at 15 kV accelerating potentional, 20 nA beam current and 3–5 μm beam diameter for analyses of garnet, amphiboles, and diopside, and 15 kV, 10 nA and 10–15 μm for analyses of micas, chlorite, pumpellyite, prehnite, and feldspar. The following standards were used: synthetic SiO_2 (Si$K\alpha$), TiO_2 (Ti$K\alpha$), Al_2O_3 (Al$K\alpha$), metallic V (V$K\alpha$), chromite (Cr$K\alpha$), hematite (Fe$K\alpha$), rhodonite (Mn$K\alpha$), MgO (Mg$K\alpha$), wollastonite (Ca$K\alpha$), barite (Ba$L\alpha$), albite (Na$K\alpha$), and orthoclase (K$K\alpha$). The EMP detection limit for the measured elements was 0.05 to 0.1 wt%. The measurement accuracy varied between ±0.1 to 0.5 wt% under optimal operating conditions. For data processing, the overlap correction and PAP routine of Pouchou and Pichoir (1985) was used.

Data were collected on garnet with a Philips PW 1710 X-ray diffractometer at the Geological Institute, Slovak Academy of Sciences, Bratislava. Cu$K\alpha$ was used, with instrumented conditions of 35 kV voltage, 20 nA current, and a 0.3 °2θ/min goniometer speed. Lattice parameters were calculated using the unit-cell software of Holland and Redfern (1997).

The crystal structure of a birefringent garnet was studied by single-crystal X-ray diffraction. The sample was shaped to an ellipsoid with the main radii of 0.125, 0.125, and 0.15 mm using a compression air grinder. Room-temperature diffraction data (28206 reflections with $-13 \le h \le 13$, $-15 \le k \le 14$, $-14 \le l \le 14$, $2\Theta_{max} = 53.43°$) were collected on a Bruker AXS Kappa X8 APEX II X-ray autodiffractometer (Mo$K\alpha$ radiation, graphite monochromator) equipped with a CCD detector.

Results

Petrography and rock composition

The host rocks are fine- to medium-grained, dark-gray schists (commonly named black schists) with varying amounts

of primary clastic and tuffaceous mafic components. The rocks have a fine-grained groundmass with larger porphyroblastic aggregates of amphibole, garnet, pyroxene, plagioclase, pyrite, and several other minerals. Due to a systematic black carbon admixture, they could be referred to as C-rich amphibole schists with pyrite ± pyrrhotite.

The groundmass is very fine grained with visible metamorphic foliation and lepidogranoblastic to nematoblastic texture (see Fig. 5c, later in this paper). Due to the small size of the crystals (mainly 20 to 100 μm), as well as the common presence of opaque black carbon particles, the minerals of the groundmass were difficult to distinguish under the optical microscope. Therefore, they were studied using back-scattered electron (BSE) imaging and EMPA. The groundmass (see Fig. 5c, later in this paper) consists of albite (±plagioclase), quartz, amphibole, phlogopite, chlorite, muscovite, pumpellyite, titanite, and pyrite. Carbonaceous matter mainly has an organic origin and has been metamorphosed to the metaanthracite-semigraphite stage with low contents of bitumen (Cambel et al. 1985; Molák and Slavkay 1996). The C-rich amphibole schists show a large compositional variability, mainly in Fe, Mg, Ca, Na, and K, but generally they are Al-depleted and enriched in V, Cr, Ni, Co, and Cu (Table 1).

Mineral description

The garnet belongs to goldmanite-grossular-uvarovite solid-solution series, with the goldmanite end-member predominating (Uher et al. 1994). The green garnet was originally called "uvarovite" when it was discovered in the Rybníček deposit near Pezinok (Čillík et al. 1959). It takes the form of dark emerald-green, semi-transparent crystals with {110} and more rarely {221} crystal faces. Fresh surfaces have a slight glassy luster, whereas weathered crystals and aggregates are pale green (Fig. 2a). The size of the crystals is typically 1–2 mm, rarely up to 5 mm; aggregates can reach up to 2 cm in size. Under the microscope, it is pale green with a distinct anomalous birefringence characterized by irregular optical domains (Fig. 2b). The garnet is associated with amphibole, pyrite, pyrrhotite, albite (Figs. 2c–2d), and commonly contains inclusions of pyrite/pyrrhotite and carbonaceous matter. Locally, garnet crystals show a skeletal atoll-like shape in association with tremolite (amphibole I) and albite (Fig. 2d).

TABLE 1. Representative chemical analyses of C-rich amphibole schists from the PPCC

Sample no.	RY-1	MI-1	62 A
Locality	Pezinok, Rybníček adit	Pezinok, Michal adit	Pezinok, Cajla mine
SiO_2	53.42	54.64	60.51
TiO_2	0.28	0.21	0.37
Al_2O_3	11.42	5.68	6.54
FeO_{total}	4.85	18.32	10.59
MnO	0.05	0.05	0.06
MgO	6.61	1.84	2.89
CaO	11.26	4.08	4.61
Na_2O	3.09	0.94	0.75
K_2O	0.10	0.05	1.08
P_2O_5	0.27	0.32	n.a.
C_{org}	n.a.	n.a.	4.90
L.O.I.	8.20	13.88	6.15
Total	99.55	100.01	98.45
V	1150	770	720
Cr	760	224	60
Ni	60	1080	288
Co	57	17	19
Cu	229	300	209
U	n.a.	n.a.	24
Sr	19	43	49
Ba	575	1910	470

Notes: Main elements and organic carbon (C_{org}) in wt%, trace elements in ppm; RY-1 and MI-1 (this work), 62 A (Cambel and Khun 1983). The compositions determined by XRF (main elements), conductometry (C_{org}) and optical spectroscopy (OES); analytical conditions as Cambel and Khun (1983).

EMPA reveals strong variations in V, Cr, and Al, i.e., within goldmanite-uvarovite-grossular solid solutions (Fig. 3). These analyses show 5–19 wt% V_2O_3, 5–11 wt% Cr_2O_3, and 2–13 wt% Al_2O_3, corresponding to 16–64 mol% goldmanite, 19–36 mol% of uvarovite, and 9–59 mol% of grossular (Table 2; Fig. 3). The largest compositional variations are between V and Al. The V/Cr atomic ratio varies only slightly (ca. 2.5–3). The V, Cr, and Al contents of garnet are characteristic for each of the studied localities. For example, garnet from Lower Augustín a Michal adits has the highest V contents (up to 22 wt% V_2O_3 or 73 mol% goldmanite), whereas garnet from the Rybníček and especially Lower Augustín adits have the highest Al contents (up to 13 wt% Al_2O_3 or 59 mol% grossular) and the lowest V contents (5 wt% V_2O_3 or 16 mol% goldmanite). Uvarovite-dominant compositions with 10 wt% Cr_2O_3, 9.5 wt% V_2O_3, and 7.5 wt% Al_2O_3 (34 mol% uvarovite, 32 mol% goldmanite, and 33 mol% grossular end-member) were formerly described only in Rybníček (Uher et al. 1994). The garnet is unzoned or shows V-rich cores and Al-rich rims or irregular coarse oscillatory zoning with variations in V, Cr, and Al (Fig. 4). Irregular variations in Ca and Mn are also present (Table 2).

The measured cell dimension of the garnet is in the range of 12.001(1)–12.043(1) Å, which is consistent with published data for goldmanite (Moench and Meyrowitz 1964; Strens 1965; Filippovskaya et al. 1972; Litochleb et al. 1985; Benkerrou and Fonteilles 1989; Hallsworth et al. 1992) as well as with our older data for goldmanite from Rybníček [11.969(1)–12.000(6) Å; Uher et al. 1994].

To evaluate the origin of anomalous birefringence, the crystal structure of one sample was studied using the single-crystal XRD method. Although the measured unit-cell dimensions [a = 12.003(4) Å, b = 11.991(5) Å, c = 12.009(5) Å, α = 90.12(3)°, β = 90.04(3)°, γ = 90.04(3)°] were close (within 4σ) to the ideal cubic one, the presence of anomalous birefringence, differences in the intensities of equivalent reflections, and the appearance of forbidden reflections pointed to a triclinic symmetry typical for natural Ca garnets (Wildner and Andrut 2001; Shtukenberg et al. 2005 and references therein). Refinement of the crystal structure was performed using the SHELXL program package (Sheldrick 1997) for the ideal cubic space group $Ia\bar{3}d$ [R = 0.0244 for 149 unique reflections with $F_o > 4\sigma(F_o)$, R_w = 0.0633] as well as in the triclinic space group $I\bar{1}$ [R = 0.0534 for 2533 unique reflections with $F_o > 4\sigma(F_o)$, R_w = 0.1744]. The high R-value obtained for the triclinic space group did not allow for it to be preferred it to the cubic one. As a consequence, the final atomic coordinates are presented for the cubic variant only (Tables 3 and 4).

The data agree with the general formula $Ca_3M_2(SiO_4)_3$ where the M site is occupied by Al, V, and Cr. Unfortunately, XRD is unable to distinguish which of the three different cations occupies the M site without constraints on the crystal composition.

Table 2. Representative compositions of silicate minerals from C-rich amphibole schists of the PPCC (wt%)

Mineral	goldmanite	goldmanite	goldmanite	grossular	grossular	grossular	amphibole I	amphibole I	amphibole I_{Ed} edenite	amphibole II	diopside	diopside
Locality	Rybníček	Rybníček	Augustín	Rybníček	Rybníček	Augustín	Rybníček	Rybníček	Rybníček	Augustín	Rybníček	Rybníček
Sample	RY127	RY124	DA1112	RY134	RY135	DA118	RY13	RY626	RY423	DA4a	RY14a	RY110
SiO_2	35.85	37.17	36.63	37.46	37.29	38.23	50.98	56.58	48.07	54.67	54.38	54.13
TiO_2	0.00	0.00	0.32	0.03	0.22	0.00	0.00	0.00	0.99	0.00	0.00	0.00
Al_2O_3	2.02	6.76	4.09	8.69	8.69	10.68	7.59	2.56	11.64	2.86	2.31	1.39
V_2O_3	18.93	14.59	16.15	10.19	6.98	6.10	2.58	0.65	0.00	0.00	0.40	1.01
Cr_2O_3	8.36	6.15	8.24	8.20	11.39	9.01	0.64	0.00	0.00	0.00	0.00	0.42
FeO	0.13	0.20	0.00	0.34	0.51	0.56	0.25	0.26	0.20	5.10	2.37	0.00
MnO	0.75	1.42	1.37	2.36	2.89	4.32	0.00	0.00	0.00	1.83	0.00	0.00
MgO	0.00	0.09	0.00	0.04	0.02	0.29	21.12	23.46	21.22	18.96	16.50	17.17
CaO	33.42	33.59	33.51	32.88	32.15	31.09	12.81	13.50	13.44	12.54	23.47	24.57
BaO												
Na_2O							1.40	0.35	2.20	0.63	0.52	0.98
K_2O							0.00	0.15	0.18	0.00	0.08	0.00
H_2O (calculated)							2.16	2.20	2.17	2.12		
Total	99.46	99.97	100.31	100.19	100.14	100.28	99.53	99.71	100.11	98.71	100.03	99.67
Number of O atoms	12	12	12	12	12	12	23	23	23	23	6	6
Si	2.977	3.001	2.986	3.000	2.993	3.034	7.063	7.720	6.634	7.737	1.970	1.965
Ti	0.000	0.000	0.020	0.002	0.013	0.000	0.000	0.000	0.103	0.000	0.000	0.000
Al	0.198	0.643	0.393	0.820	0.822	0.999	1.239	0.412	1.893	0.477	0.099	0.059
V	1.260	0.945	1.055	0.654	0.449	0.388	0.287	0.071	0.000	0.000	0.012	0.029
Cr	0.549	0.393	0.531	0.519	0.723	0.565	0.070	0.000	0.000	0.000	0.000	0.012
Fe	0.008	0.012	0.000	0.021	0.031	0.033	0.029	0.030	0.023	0.604	0.072	0.000
Mn	0.053	0.097	0.095	0.160	0.197	0.290	0.000	0.000	0.000	0.219	0.000	0.000
Mg	0.000	0.011	0.000	0.005	0.002	0.034	4.362	4.772	4.366	4.000	0.891	0.929
Ca	2.974	2.906	2.926	2.821	2.765	2.644	1.901	1.974	1.987	1.901	0.911	0.956
Ba												
Na							0.376	0.093	0.589	0.173	0.037	0.069
K							0.000	0.026	0.032	0.000	0.004	0.000
Total	8.019	8.008	8.006	8.002	7.995	7.987	15.327	15.098	15.627	15.111	3.996	4.019
$Mg/(Mg + Fe^{2+})$							0.993	0.994	0.995	0.869	0.925	1.000

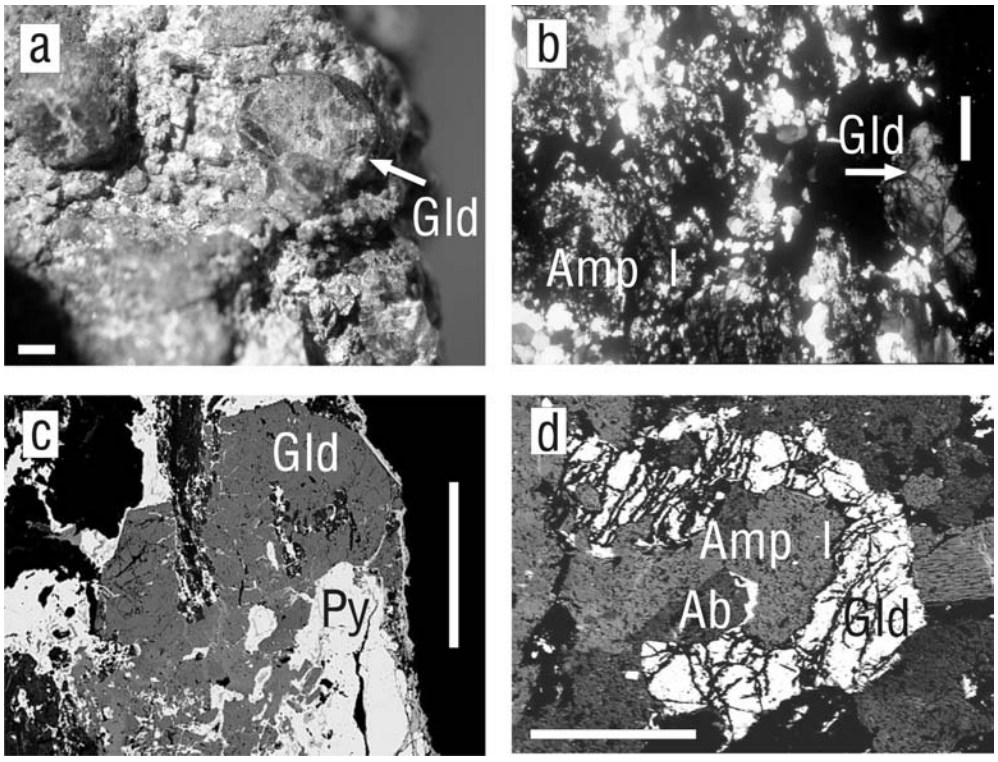

Figure 2. Garnet (goldmanite-grossular-uvarovite s.s.) from C-rich amphibole schists. (**a**) Crystal morphology. (**b**) Birefringence of garnet (Gld) in amphibole-quartz-pyrite/pyrrhotite-bearing metabasic pyroclastic rock (crossed polars). (**c**) Garnet (Gld) in association with pyrite/pyrrhotite (Py, white areas) and silicate minerals (dark gray to black), BSE image. (**d**) Atoll-shaped garnet (white areas) with amphibole I (Amp I) and albite (Ab), BSE image. (**a**–**c**) Rybníček adit, (**d**) Lower Augustín adit. Scale bars on each image represent 500 μm.

TABLE 2. —*Continued*

Mineral	mukhhinite	chromian clinozoisite	clinozoisite I	clinozoisite II	muscovite I	muscovite I	muscovite II	muscovite II	phlogopite	clinochlore	pumpellyite -(Mg)	prehnite
Locality	Rybníček	Rybníček	Rybníček	Rybníček	Rybníček	Augustín	Rybníček	Rybníček	Rybníček	Rybníček	Rybníček	Rybníček
Sample	RY612	RY106	RY1-5Z	RY116	RY12M	HA2-11S	1bM41	RY606	RY427	RY404	RY69	RY519
SiO_2	36.81	37.43	39.05	39.10	44.73	45.29	47.58	46.42	39.18	31.81	36.74	43.34
TiO_2	0.00	0.00	0.00	0.00	0.69	1.96	0.27	0.00	2.16	0.60	0.00	0.00
Al_2O_3	23.25	22.70	27.24	30.59	23.09	29.04	33.14	29.52	17.77	19.83	25.97	25.28
V_2O_3	8.10	1.88	5.78	0.00	7.50	5.61	0.00	0.00	0.00	0.00	0.00	0.00
Cr_2O_3	4.60	11.28	0.70	0.00	6.93	0.39	0.00	0.00	0.22	0.24	0.17	0.00
FeO	0.70	1.00	0.54	3.19	0.00	0.00	0.00	1.16	0.75	4.12	2.34	0.26
MnO	0.00	0.68	0.00	0.00	0.00	0.00	0.00	0.00	0.00	0.18	0.44	0.00
MgO	0.20	0.00	0.49	0.29	2.17	2.57	2.42	3.76	24.29	31.03	3.16	0.49
CaO	23.31	22.68	23.50	23.58	0.00	0.00	0.00	0.25	0.00	0.00	23.52	26.27
BaO					0.00	0.00	0.00	3.19	0.00			
Na_2O	0.00	0.00	0.13	0.11	0.15	0.23	0.08	0.28	0.36	0.00	0.00	0.23
K_2O	0.00	0.09	0.00	0.00	10.48	10.29	11.23	9.99	9.68	0.00	0.08	0.21
H_2O (calculated)	1.87	1.88	1.93	1.93	4.32	4.43	4.50	4.35	4.27	12.83	7.59	4.38
Total	98.84	99.62	99.36	98.79	100.06	99.81	99.22	98.92	98.68	100.64	100.01	100.46
Number of O atoms	12.5	12.5	12.5	12.5	11	11	11	11	11	14	12	11
Si	2.954	2.992	3.041	3.040	3.102	3.062	3.172	3.196	2.751	2.974	2.903	2.964
Ti	0.000	0.000	0.000	0.000	0.036	0.100	0.014	0.000	0.114	0.042	0.000	0.000
Al	2.199	2.138	2.500	2.803	1.887	2.314	2.604	2.395	1.471	2.185	2.418	2.038
V	0.521	0.120	0.361	0.000	0.417	0.304	0.000	0.000	0.000	0.000	0.000	0.000
Cr	0.292	0.713	0.043	0.000	0.380	0.021	0.000	0.000	0.012	0.018	0.011	0.000
Fe	0.047	0.067	0.035	0.207	0.000	0.000	0.000	0.067	0.044	0.322	0.155	0.015
Mn	0.000	0.046	0.000	0.000	0.000	0.000	0.000	0.000	0.000	0.014	0.029	0.000
Mg	0.024	0.000	0.057	0.034	0.224	0.259	0.241	0.386	2.543	4.326	0.372	0.050
Ca	2.004	1.942	1.961	1.965	0.000	0.000	0.000	0.018	0.000	0.000	1.991	1.925
Ba					0.000	0.000	0.000	0.086	0.000			
Na	0.000	0.000	0.020	0.017	0.020	0.030	0.010	0.037	0.049	0.000	0.000	0.031
K	0.000	0.009	0.000	0.000	0.927	0.888	0.955	0.877	0.867	0.000	0.008	0.018
Total	8.041	8.027	8.018	8.066	6.994	6.978	6.995	7.064	7.851	9.881	7.887	7.041
$Mg/(Mg+Fe^{2+})$									0.983	0.931	0.706	

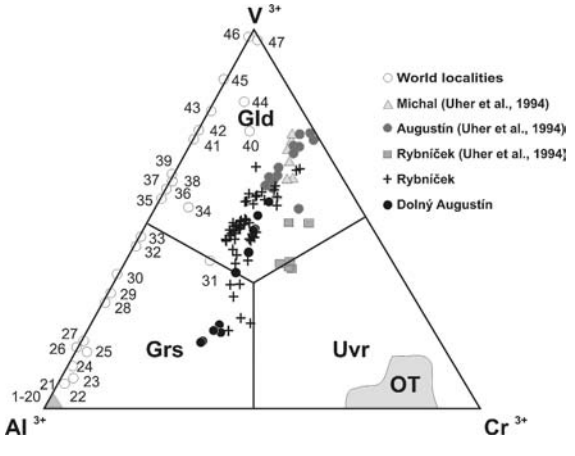

FIGURE 3. Ternary V-Al-Cr diagram (atomic proportions) of garnet from C-rich amphibole schists of the PPCC in comparison to the world occurrences (1 to 47, for locality explanations see Uher et al. 1994). Abbreviations of compositional fields: OG = Ogcheon belt, Korea (Jeong and Kim 1999); PB = Poblet area, Spain (Canet et al. 2003); OT = V-bearing uvarovite from Outolumpu, Finnland (von Knorring et al. 1986).

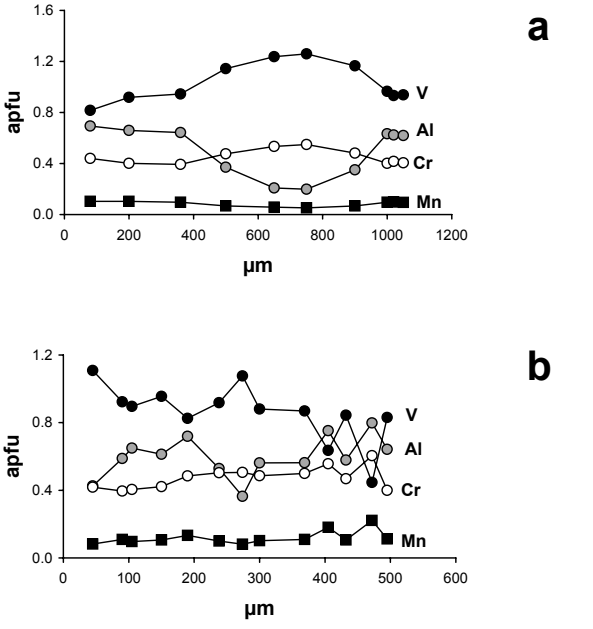

FIGURE 4. Compositional profiles through garnet crystals from C-rich amphibole schists of the PPCC.

Therefore, initially the M site was assumed to be occupied by Al and V. Crystal structure refinement gave the composition of the M site as $Al_{0.27(1)}V_{0.73(1)}$ (i.e., ~20.3 electrons per site). Since V and Cr have nearly the same atomic scattering factors, the amount of Al should be close to the true value. EMPA data show that the atomic V/Cr ratio is nearly constant (see above) and equal to approximately 2, for a sample composition of $Ca_3(Al_{0.29(1)}V_{0.47(1)}Cr_{0.24(1)})_2(SiO_4)_3$. The crystal structure is very close to that of goldmanite $Ca_3(Al_{0.24}V_{0.6}Fe_{0.16})_2(SiO_4)_3$ (Novak

TABLE 3. Fractional atomic coordinates and isotropic displacement parameters U_{eq} of the garnet crystal structure refined in the space group $Ia\bar{3}d$ (Rybníček adit)

Site	*x/a*	*y/b*	*z/c*	U_{eq} (Å^2)
M	0	0	0	0.0068(5)
Ca	0	0.25	0.125	0.0094(4)
Si	0	0.25	0.375	0.0086(5)
O	0.03912(14)	0.04763(13)	0.65442(13)	0.0100(6)

TABLE 4. Anisotropic displacement parameters, U_{ij} (Å^2) of the garnet crystal structure refined in the space group $Ia\bar{3}d$ (Rybníček adit)

Site	U_{11}	U_{22}	U_{33}	U_{23}	U_{13}	U_{12}
M	0.0068(5)	U_{11}	U_{11}	0.0003(2)	U_{11}	U_{11}
Ca	0.0106(5)	U_{11}	0.0070(6)	0	0	0.0013(3)
Si	0.0092(6)	U_{11}	0.0075(7)	0	0	0
O	0.0122(10)	0.0090(10)	0.0089(9)	0.0007(7)	–0.0002(7)	0.0003(6)

and Gibbs 1971).

Despite the unclear result obtained for refinement in the triclinic space group $I\bar{1}$, cation ordering seems, nevertheless, to be present in this sample. This conclusion is supported by the different compositions on the eight octahedral M sites, which are independent in the space group $I\bar{1}$. Their occupancy by Al (the rest was assumed to be V) was found to be as follows: 0.24(1), 0.25(1), 0.27(1), 0.24(1), 0.21(1), 0.36(1), 0.35(1), and 0.37(1). These values are consistent with average <M-O> bond lengths equal to 1.998(3), 1.994(3), 1.994(3), 1.998(3), 1.999(3), 1.988(3), 1.993(3), and 1.992(3) Å, respectively. We believe that the high *R*-value obtained for the triclinic space group results from the low quality of the sample, probably due to the small size of the original crystal and the possible existence of several growth sectors. All of these sectors would have contributed to the diffraction pattern providing an incorrect result. The ordering of the M cations has been detected in other studies for grossular-andradite and grossular-uvarovite solid solutions (Takéuchi et al. 1982; Wildner and Andrut 2001; Shtukenberg et al. 2005 and references therein). The present study shows that ordering is also possible for solid solutions with a significant goldmanite component. Referring to other ugrandite garnets, this ordering seems to originate from the growth ordering of atoms or a growth dissymmetrization phenomenon, which presumably are the cause of the anomalous birefringence (Akizuki 1984; Shtukenberg et al. 2002, 2005).

Amphiboles are the most common porphyroblasts. They form aggregates and more rarely, individual euhedral to subhedral crystals. The average size of the amphibole crystals is in the range from 0.1 to 5 mm, in some cases up to 15 mm. Folded relicts of C-rich matter included in the amphibole porphyroblasts indicate their late- to post-kinematic metamorphic origin. Textural relationships and EMPA reveal several amphibole populations (Figs. 2d, 5a, 5b, 5e, and 6; Table 2).

Amphibole I is the most common type, forming porphyroblasts in association with diopside (Figs. 5a–5b). Amphibole I is colorless or rarely pale green without visible pleochroism. It is classified as tremolite to magnesiohornblende (Leake et al. 1997) with nearly pure Mg end-members composition: [Mg/(Mg + Fe) = 0.95–1 (Table 2; Fig. 6a)]. Commonly, elevated V and Cr contents of up to 2.6 wt% V_2O_3 (0.3 V apfu) and up to 0.9 wt% Cr_2O_3 (0.1 Cr apfu) occur in amphibole I; Al_2O_3 contents range between 1.2 and 7.6 wt%. Rarely, amphibole I is altered along cleavage planes to an aggregate of late fine-grained clinozoisite, muscovite, and pumpellyite.

Amphibole I_{Ed} (edenite-rich amphibole) occurs rarely in association with amphibole I porphyroblasts, forming smaller euhedral to subhedral crystals up to 0.5 mm in size. Amphibole I_{Ed} could be classified as edenite according to the nomenclature of Leake et al. (1997) despite the relatively low Na content [1.7–2.2 wt% Na_2O, 0.45–0.59 Na apfu, ^{A}(Na+K) = 0.50–0.62 apfu] compared to the edenite end-member. The edenite has a very high Mg/Fe ratio [Mg/(Mg + Fe) = 0.99–1], a lower Si content (48.1 – 48.5 wt% SiO_2, 6.63–6.74 Si apfu), and a higher total Al content (9.7–11.6 wt% Al_2O_3, 1.59–1.89 Al apfu) in comparison to the other studied amphiboles (Table 2; Fig. 6b). The studied edenite is V-poor, but it contains up to 1.5 wt% Cr_2O_3.

Amphibole II forms rare small subhedral to anhedral crystals (up to 0.1 mm in size) that locally replace amphibole I and diopside and is in close association with a younger generation of albite. Amphibole II compositions lie near the actinolite-tremolite boundary with Mg/(Mg + Fe) = 0.84 – 0.92 (Fig. 6a). Aluminum contents (0.8–2.9 wt% Al_2O_3) are lower in comparison to amphibole I. Neither V nor Cr were detected (Table 2). Generally, the distribution of V and Cr in all the amphiboles is irregular without any systematic distribution within the crystal. The V^{3+} and Cr^{3+} cations are located on the C-position in the amphibole together with Al^{3+} as part of the coupled subtitution $^C(Mg,Fe^{2+})$ ^TSi $^C(Al,V,Cr)_{-1}$ $^TAl_{-1}$.

Diopside is less common but characteristic of the peak metamorphic stage for these rocks. It forms anhedral to subhedral grains, rarely euhedral columnar crystals, up to 0.5 mm in length. In many cases, diopside overgrows amphibole I, but locally diopside relics in amphibole were also identified (Fig. 5b). Locally, diopside appears in spatial relation with albite. Quartz-calcite veinlets with diopside also occur. This phenomenon indicates a partly metasomatic origin for the diopside, connected with a fluid influx, probably associated with the Modra tonalite-granodiorite contact aureole. EPMA indicates a nearly pure diopside composition, with up to 2.5 wt% Al_2O_3, 1.7 wt% V_2O_3, 0.4 wt% Cr_2O_3, and 2.5 wt% FeO (Table 2).

Plagioclase is a characteristic phase of the groundmass (Fig. 5c); locally both nearly pure albite and a rare intermediate plagioclase ($An_{39–47}$) occur together. The co-existence of both plagioclase compositions seems to be the result of disequilibrium conditions during a relatively short-term contact-thermal metamorphic event. Moreover, near end-member albite ($Ab_{93–98}$ $An_{2–5}Or_{0–2}$) forms anhedral to subhedral crystals, 0.1–0.3 mm in size, in association with garnet, diopside, clinozoisite I, and amphibole (Figs. 2d, 5a, 5d, and 5e). Some of the albite may have formed during more recent retrograde metamorphism.

Clinozoisite forms anhedral porphyroblasts (up to 0.5 mm in size) or fine-grained aggregates. Porphyroblasts (clinozoisite I) are commonly zoned and show a greenish pleochroism. This clinozoisite is syngenetic to slightly younger diopside. Microscopic observations indicate that clinozoisite I and amphibole I (tremolite) are not found together. Clinozoisite I, in many cases, crystallized with diopside, but tremolite is always associated with diopside, not with clinozoisite I (Figs. 5a and 5d). Clinozoisite I contains 2.1–9.5 wt% V_2O_3 and 1.4–11.3 wt% Cr_2O_3

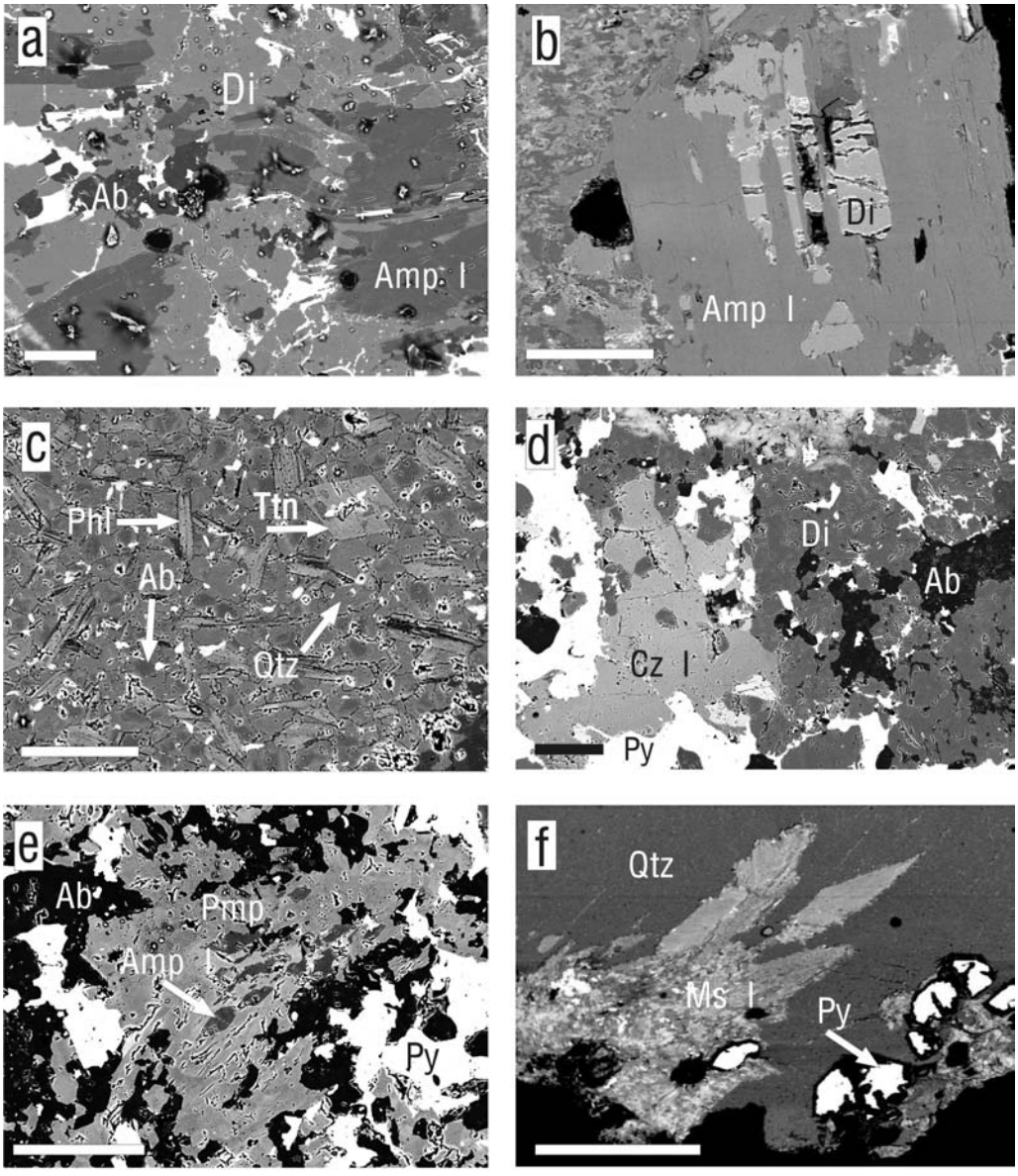

Figure 5. BSE images of metamorphic assemblage from C-rich amphibole schists of the PPCC. (**a**–**e**) Rybníček adit. (**f**) Upper Augustín adit. Abbreviations: Ab = albite, Amp I = amphibole I, Cz I = V,Cr-rich clinozoisite, Di = diopside, Ms I = V,Cr-rich muscovite I, Phl = phlogopite, Pmp = pumpellyite-(Mg), Py = pyrite/pyrrhotite, Ttn = titanite. Scale bars on each image represent 100 μm.

(0.13–0.62 V apfu and 0.09–0.71 Cr apfu, respectively). Some compositions reach mukhinite and "chromian clinozoisite" compositions (Table 2; Fig. 7). The compositions with V > (Al,Cr) in the M3 position belong to mukhinite, whereas one Cr-rich composition (0.713 Cr apfu, Table 2) indicates the presence of a Cr-dominant member in the M3 position (Fig. 7). However, preliminary structural results for Cr-rich clinozoisite or epidote (called "tawmawite"), from Outokumpu, Finnland, indicate that Cr is disordered over the M3 and M1 positions. This finding casts doubt on the validity of the Cr-dominant member if Cr < 1 apfu. The name chromian (or Cr^{3+}-rich) clinozoisite is preferred until new evidence is presented (Armbruster et al. 2006). Fine-grained clinozoisite II, without V and Cr, is the product of retrograde low-temperature metamorphism together with V,Cr-free clinochlore, pumpellyite-(Mg), muscovite II, and possibly albite II.

Muscovite forms subhedral, lamellar, greenish crystals, up to 1 mm in size, in association with amphibole I, quartz I, and pyrite/pyrrhotite (Fig. 5f) or tiny, up to 0.1 mm, subhedral to anhedral, colorless crystals in the groundmass, which reflects the original clay content of the source rocks. Two muscovite generations are recognized: V,(Cr)-rich muscovite I with 2.5–8 wt% V_2O_3 and 0–7 wt% Cr_2O_3 (0.12–0.45 and up to 0.39 apfu V and Cr, respectively) and V,Cr-free muscovite II with ≤0.4 wt% V_2O_3 and Cr_2O_3 (Table 2; Fig. 8). VAl_{-1} and $CrAl_{-1}$ are the most evident substitution mechanisms in muscovite I (Fig. 8). Locally, Ba-rich muscovite II was detected (Table 2). Vanadium,(Cr)-rich

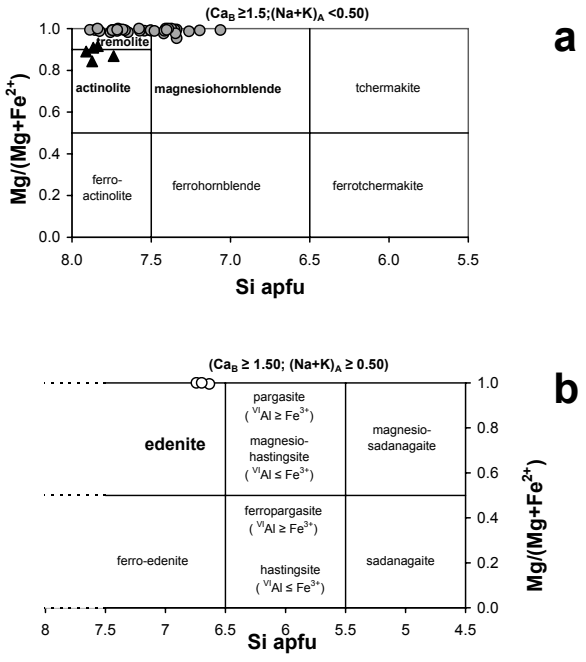

Figure 6. Amphibole compositions from C-rich amphibole schists of the PPCC. (**a**) Amphibole I (gray circles), amphibole II (black triangles). (**b**) Amphibole I, edenite (open circles).

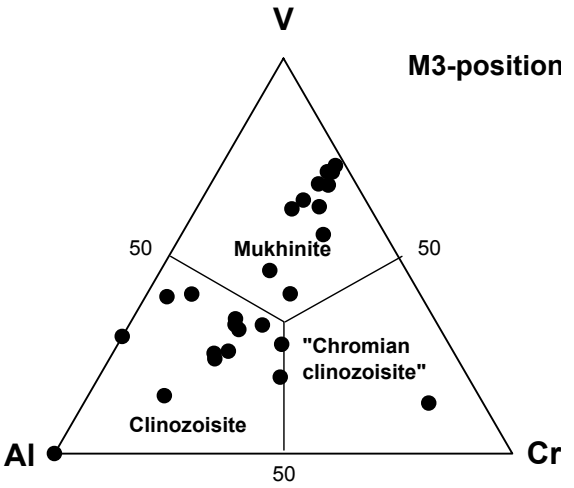

Figure 7. Ternary V-Al-Cr diagram of epidote group minerals from C-rich amphibole schists of the PPCC.

muscovite I formed during high-grade contact metamorphism together with garnet, amphibole, diopside, and V,Cr-rich clinozoisite I, whereas V,Cr-free muscovite II is related to younger, retrograde processes.

Phlogopite of nearly pure Mg composition [Mg/(Mg + Fe) = 0.97–0.98: Table 2], is closely associated with clinochlore in some samples (Fig. 5c). In rare cases, phlogopite forms fan-like aggregates up to 0.5 mm in size. The crystallization of phlogopite is probably connected with the formation of diopside, garnet, and both amphibole generations.

Chlorite is non-pleochroic with gray interference colors, and corresponds to the Mg end-member clinochlore with Mg/(Mg + Fe) = 0.93–0.98 (Table 2). Clinochlore is syngenetic to slightly younger phlogopite. Crystallization of chlorite, like albite, was probably the product of manifold metamorphic events; both during contact metamorphism as well as during secondary alteration.

Titanite forms small euhedral to subhedral crystals in the groundmass (Fig. 5c) as well as in association with diopside, albite, clinozoisite I, and pyrite/pyrrhotite. Fluorapatite forms as rare, anhedral, 20–35 μm grains in association with amphibole I and diopside porphyroblasts.

Pumpellyite occurs as a typical alteration product of the groundmass and porphyroblasts. Locally zoned pumpellyite, in association with albite, replaces diopside and amphibole I (Fig. 5e). It forms scarce fine, fan-shaped aggregates. EMPA reveal pumpellyite-(Mg) compositions [Mg/(Mg + Fe) = 0.70–0.99], to be relatively enriched in Al (Table 2). Prehnite is a rare phase and forms subhedral grains (up to 0.1 mm) in association with clinozoisite II. It shows a nearly pure end-member composition (Table 2). Anhedral quartz grains and aggregates are found in the groundmass or form late hydrothermal veinlets and quartz-rich zones.

Calcite forms interstitial grains scattered in the groundmass (up to 0.3 mm large) or irregular veinlets and domains with quartz. Primary carbonates were not detected in the groundmass. The presence of calcite and siderite in these rocks is probably related to the influence of younger, granite-related, post-magmatic, mainly hydrothermal fluids. However, the pre-metamorphic existence of minor calcite can be indirectly assumed to be due to the later crystallization of Ca-bearing metamorphic silicates. Local, late hydrothermal siderite forms fine-grained aggregates or coarse-grained veinlets (up to 3 mm thick) associated with quartz.

Pyrite is widespread. It forms euhedral to subhedral hexahedric crystals in the groundmass and 0.01–5 mm crystals in association with amphiboles, diopside, garnet, and pyrrhotite. In some cases, subhedral pyrite forms 0.1–0.2 mm large inclusions in goldmanite. Small pyrite crystals and fine-grained aggegates are an inseparable part of the primary rock composition and locally form a stratiform pyrite mineralization. However, the larger pyrite crystals are likely to have formed with other porphyroblastic phases in the course of later metamorphic events.

Irregular, fine-grained pyrrhotite aggregates (usually up to 5 cm in size) are common locally. Pyrrhotite is associated with amphiboles, garnet, quartz, and pyrite. Crystallization and/or recrystallization of the Fe sulfide stratiform mineralization may have occurred over a wide time span ranging from diagenesis to metamorphism and remobilization during late hydrothermal alteration. Rare chalcopyrite forms anhedral grains (up to 15 μm in size) in association with late siderite and quartz veinlets. Rare, subhedral to anhedral uraninite grains, 5–25 μm in size, were detected at the contact of pyrrhotite and unspecified silicate minerals in the Rybníček adit (Cambel et al. 1977).

Petrogenetic evolution of V-Cr mineralization: interpretation and discussion

Vanadium-rich silicate mineralizations have been described in a series of localities. These consist of goldmanite (or V-rich garnet) and/or V-rich micas, amphiboles, pyroxenes, clinozoisite,

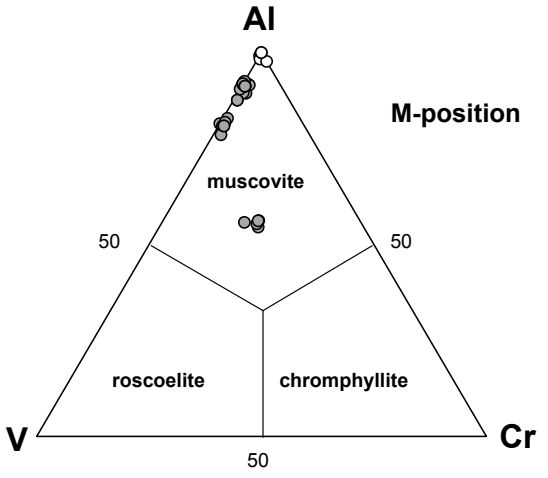

Figure 8. Ternary Al-V-Cr diagram of mica group minerals from C-rich amphibole schists of the PPCC; muscovite I (gray circles), muscovite II (open circles).

titanite, spinels, and other minerals (e.g., Moench and Meyrowitz 1964; Momoi 1964; Shepel and Karpenko 1970; Filippovskaya et al. 1972; Karev 1974; Suwa et al. 1979; Benkerrou and Fonteilles 1989; Pan and Fleet 1992; Jeong and Kim 1999). However, in each of these cases, the Cr content in the minerals and rocks was usually low. On the other hand, metamorphic Cr-rich assemblages with uvarovite and other Cr-bearing silicates are commonly poor in V (e.g., Wan and Yeh 1984; von Knorring et al. 1986).

The PPCC occurrence represents a V- and Cr-rich metamorphic assemblage with goldmanite-uvarovite-grossular garnet, V,Cr-rich clinozoisite, and muscovite. Such V,Cr-rich metamorphic assemblages are very rare. Chromian goldmanite with other V-(Cr)-enriched silicates (titanite, allanite, biotite, amphiboles) and variegated V-Cr oxide minerals occur in metasedimentary rocks of the Poblet area, Spain (Canet et al. 2003). Somewhat elevated Cr and Ti contents are reported in vanadian grossular to spessartine from the Domoradice graphite deposit, Czech Republic ($Grs_{23–49}Sps_{27–49}$: 0–7.5 mol% uvarovite, 0.5–3.6 mol% schorlomite and 0.2–25.6 mol% goldmanite; Černý et al. 1995). Lastly, chromian hercynite with vanadoan sillimanite have been described in V,Cr-rich metapelites from the Wind River Range, Wyoming (Donohue and Essene 2005).

The origin of a V- and Cr-rich mineral association in the PPCC can be outlined in terms of the volcano-sedimentary source material and subsequent metamorphic processes. The host rock is composed mainly of submarine basaltic rocks. Abundant organic carbonaceous matter, muscovite, and local quartz represent the main non-volcanic components. Laminated arrangement of inert carbonaceous matter marks the primary tuffaceous layers of the rocks. The presence of the mafic pyroclastic rocks with an organic admixture caused a strong effect on the precipitation of Fe sulfides in an euxinic environment. Abundant pyrite and pyrrhotite formed disseminated crystals or sulfide-rich stratiform beds, as well as local small SEDEX-type pyrite deposits in the "productive zones" of the PPCC (Cambel 1958; Cambel et al. 1977). We assume that pyrite and pyrrhotite mineralization extracted the majority of the Fe from the primary host rock, which led to the distinctive enrichment of Mg in the associated mafic silicate minerals and their metamorphic products.

The V-rich metamorphic rocks of the PPCC are closely related to the high organic carbon content. The carbon-rich schists contain, on average, around 2 wt% C_{org}, 500 ppm V, 100 ppm Cr, 180 ppm Ni, 140 ppm Cu, and 3500 ppm Ti; and locally, up to 6000 ppm V, 1000 ppm Cr, 850 ppm Ni, 530 ppm Cu, and 1 wt% Ti (Table 1; Cambel and Khun 1983). Similar V enrichment and the presence of vanadian garnet and other V-rich silicates has been reported from several C-rich ("black shale") lithologies worldwide (e.g., Filippovskaya et al. 1972; Karev 1974; Litochleb et al. 1985; Benkerrou and Fonteilles 1989; Jeong and Kim 1999; Canet et al. 2003). However, at least a fraction of the V, as well as a main portion of the Cr source originated from the mafic material of the volcanoclastic rocks.

After sedimentation and lithification of the V- and Cr-rich volcano-sedimentary protolith, a complex metamorphic evolution led to the formation of the described mineral association. Three principal metamorphic events can be recognized in the petrogenetic evolution of the V-Cr mineralization in the PPCC (cf. Buday et al. 1962; Korikovsky et al. 1984): (M1) Early Hercynian regional metamorphism of the source material; (M2) Late Hercynian contact thermal metamorphism; (M3) Retrograde effects of M2 and/or Alpine metamorphism.

During the early Hercynian, low-grade greenschist-facies metamorphism (M1) resulted in a fine-grained silicate + carbonaceous matter + pyrite mineral assemblage in the mafic tuffs as well as metamorphic foliation. Subsequent intrusion of the post-kinematic, late-orogenic Modra tonalites to granodiorites into the folded Lower Paleozoic volcano-sedimentary rocks caused late Hercynian, low-pressure contact thermal metamorphism (Korikovsky et al. 1985; Cambel et al. 1989). This dominant metamorphic event (M2) overprinted the regional M1 metamorphism. The M2 event is only locally associated with deformation. The M2 stage was also accompanied by some material input supplied by fluids released from the crystallizing granitic pluton.

The peak contact M2 metamorphic conditions resulted in crystallization of amphibole, diopside, and garnet commonly enriched in V and Cr. Amphibole I porphyroblasts formed simultaneously with diopside, but peak metamorphic conditions led seemingly to the predominance of diopside. Moreover, the presence of rare edenite argues for slightly higher temperature conditions due to their higher Al and Na content in comparison to tremolite-magnesiohornblende (amphibole I) (cf. Laird 1982). Thermodynamic equilibrium was probably not reached among all of the minerals during M2 due to its short duration and the fine-grained structure of the rocks.

Diopside formation can be approximated by the reaction: tremolite + 3 calcite + quartz = 5 diopside + 3 CO_2 + H_2O (Slaughter et al. 1975). Textural and compositional relations among M2 Ca-rich phases (diopside, goldmanite-uvarovite-grossular s.s., V,Cr-rich clinozoisite I) indicate the necessity of a Ca influx or the consumption of carbonates from within the source material.

Minerals associated with the M2 stage are similar to assemblages produced during low-pressure contact thermal metamorphism of common basaltic rocks. For example, the origin of the

two amphibole phases (tremolite-magnesiohornblende and edenite) in association with plagioclase (albite and/or oligoclase to andesine), locally with epidote, chlorite, and quartz, is estimated to have occurred at temperatures between 370 and 450 °C and at least 2 kbar (cf. Maruyama et al. 1983). On the other hand, the crystallization of grossular with V-rich andradite-grossular rims from skarn veins in the Southern Cross greenstone belt, Western Australia, is constrained by the reaction clinozoisite + quartz + calcite = grossular + H_2O + CO_2 to be around 550 °C (Mueller and Delor 1991). In addition, synthetic goldmanite has been prepared experimentally at 530 °C and 3 kbar (Strens 1965).

The youngest metamorphic event M3 clearly shows a retrograde character in comparison to the M2 stage. During M3, a metamorphic association formed under prehnite-pumpellite facies conditions, which consists of phases low in V and Cr, i.e., pumpellyite-(Mg), muscovite II, clinozoisite II, and prehnite, and possibly albite II and clinochlore II. Thin hydrothermal quartz + siderite veinlets, also associated with clinozoisite II, points to remobilization during the latest postkinematic events. This event can be connected with the thermal decline of M2 or more probably with Alpine (Cretaceous) tectonometamorphic processes, that produced axinite and pumpellyite (Vrána 1966), which are only slightly higher grade than the metamorphism of the adjacent Mesozoic sediments (cf. Plašienka et al. 1993).

Acknowledgments

This work was supported by Science and Technology Assistance Agency under contract no. APVT-20-016104, by "Tectonogenesis of Paleozoic basins" scientific project (no. 801840303/130-3) granted by Slovak Ministry of Environment and by INTAS YS Fellowship program (project 2004-83-2826). We thank P. Konečný for electron microprobe assistance and H. Euler (University of Bonn, Germany) for his help in collecting X-ray diffraction data. We also thank E. Essene, J.D. Price, and D. Harlow for their constructive comments and reviews of the manuscript.

References cited

Akizuki, M. (1984) Origin of optical variation in grossular-andradite garnet. American Mineralogist, 69, 328–338.

Armbruster, T., Bonazzi, P., Akasaka, M., Bermanec, V., Chopin, C., Gieré, R., Heuss-Assbichler, S., Liebscher, A., Menchetti, S., Pan, Y., and Pasero, M. (2006) Recommended nomenclature of epidote-group minerals. European Journal of Mineralogy, 18, 551–567.

Bagdasaryan, G.P., Gukasyan, R.C., Cambel, B., and Veselský, J. (1982) The age of the Malé Karpaty Mts. granitoid rocks determined by Rb-Sr isochrone method. Geologický Zborník Geologica Carpathica, 33, 131–140.

——— (1983) The results of Rb-Sr age determination of metamorphic rocks from the Malé Karpaty Mts. metamorphic complex. Geologický Zborník Geologica Carpathica, 34, 387–397 (in Russian with English summary).

Benkerrou, C. and Fonteilles, M. (1989) Vanadian garnets in calcareous metapelites and skarns at Coat-an Noz, Belle-Isle-en-Terre (Côtes du Nord), France. American Mineralogist, 74, 852–858.

Buday, T., Cambel, B., and Maheľ, M. (1962) Explanations to geological map of Czechoslovakia, scale 1:200,000, M-33-XXXV, M-33-XXXVI, Wien-Bratislava, 248 p. Geofond, Bratislava (in Slovak).

Cambel, B. (1958) Contribution to geology of the Pezinok-Pernek crystalline complex. Acta Geologica et Geographica Universitatis Comenianae, Geologica 1, 137–166 (in Slovak).

Cambel, B. and Khun, M. (1983) Geochemical characteristics of black shales from ore-bearing complex of the Malé Karpaty Mts. Geologický Zborník Geologica Carpathica, 34, 15–44.

Cambel, B. and Planderová, E. (1985) Biostratigraphic evaluation of metasediments in the Malé Karpaty Mts. region. Geologický Zborník Geologica Carpathica, 36, 683–701.

Cambel, B., Jarkovský, J., and Krištín, J. (1977) Geochemical investigation of the main sulphidic iron minerals by electron microprobe. Veda Press, Bratislava, 320 p.

Cambel, B., Šimánek, V., and Khun, M. (1985) Study of organic matter in black shales of the Malé Karpaty Mts. crystalline complex. Geologický Zborník Geologica Carpathica, 36, 37–50.

Cambel, B., Korikovsky, S.P., Miklóš, J., and Boronikhin, V.A. (1989) Calc-silicate hornfelses (erlans and Ca-skarns) in the Malé Karpaty Mts. region. Geologický Zborník Geologica Carpathica, 40, 281–304.

Cambel, B., Kráľ, J., and Burchart, J. (1990) Isotopic geochronology of the Western Carpathian crystalline complex with catalogue of data, 184 p. Veda Press, Bratislava (in Slovak).

Canet, C., Alfonso, P., Melgarejo, J.C., and Sorge, S. (2003) V-rich minerals in contact-metamorphosed Silurian SEDEX deposits in the Poblet area, southwestern Catalonia, Spain. Canadian Mineralogist, 41, 561–579.

Černý, P., Litochleb, J., and Šrein, V. (1995) Chromian-vanadian garnets from Domoradice near Český Krumlov graphite deposit. Bulletin Mineralogicko-petrologického oddělení Národního Muzea v Praze, 3, 205–209 (in Czech).

Čillík, I., Sobolič, P., and Žákovský, R. (1959) Some remarks about tectonics of the Pezinok-Pernek crystalline complex. Geologické Práce, Zprávy, 15, 34–64 (in Slovak).

Donohue, C.L. and Essene, E.J. (2005) Granulite-facies conditions preserved in vanadium- and chromium-rich metapelites from the Paradise Basin, Wind River Range, Wyoming, U.S.A. Canadian Mineralogist, 41, 495–511.

Filippovskaya, T.B., Shevnin, A.N., and Dubakina, L.S. (1972) Vanadian garnets and hydrogarnets from Lower Paleozoic carbon- and silica-rich schists of Ishimskaya Luka (Northern Kazakhstan). Doklady Akademii Nauk SSSR, Earth Sciences Section, 203, 1173–1176 (in Russian).

Finger, F., Broska, I., Haunschmid, B., Hraško, L., Kohút, M., Krenn, E., Petrík, I., Riegler, G., and Uher, P. (2003) Electron-microprobe dating of monazites from Western Carpathian basement granitoids: Plutonic evidence for an important Permian rifting event subsequent to Variscan crustal anatexis. International Journal of Earth Sciences, 92, 86–98.

Hallsworth, C.R., Livingstone, A., and Morton, A.C. (1992) Detrital goldmanite from Palaeocene of the North Sea. Mineralogical Magazine, 56, 117–120.

Holland, T.J.B. and Redfern, S.A.T. (1997) Unit cell refinement from powder diffraction data: The use of regression diagnostics. Mineralogical Magazine, 61, 65–77.

Ivan, P., Méres, S., Putiš, M., and Kohút, M. (2001) Geochemistry of metabasalts and metasediments from the Malé Karpaty Mts. crystalline complex (Western Carpathians): Evidence for Early Paleozoic riftogeneous basin and oceanic crust. Geologica Carpathica, 52, 67–78.

Jeong, G.Y. and Kim, Y.H. (1999) Goldmanite from the black slates of the Ogcheon belt, Korea. Mineralogical Magazine, 63, 253–256.

Karev, M.E. (1974) New findings of vanadium-bearing minerals in metamorphic rocks of the Kuzneck Alatau. Geologiya i Geofizika, 11, 141–143 (in Russian).

Korikovsky, S.P., Cambel, B., Miklóš, J., and Janák, M. (1984) Metamorphism of the Malé Karpaty crystalline complex: Stages, zonality, relationship to granitic rocks. Geologický Zborník Geologica Carpathica, 35, 437–462 (in Russian).

Korikovsky, S.P., Cambel, B., Boronikhin, V.A., Putiš, M., and Miklóš, J. (1985) Phase equillibria and geothermometry of metapelitic hornfels around the Modra granitic massif (Malé Karpaty). Geologický Zborník Geologica Carpathica, 36, 51–74 (in Russian).

Laird, J. (1982) Amphiboles in metamorphosed basaltic rocks: Greenschist facies to amphibole facies. In D.R. Veblen and P.H. Ribbe, Eds., Amphiboles: Petrology and Experimental Phase Relations, 9B, p. 113–137. Reviews in Mineralogy, Mineralogical Society of America, Chantilly, Virginia.

Leake, B.E., Woolley, A.R., Arps, C.E.S., Birch, W.D., Gilbert, M.C., Grice, J.D., Hawthorne, F.C., Kato, A., Kisch, H.J., Krivovichev, V.G., Linthout, K., Laird, J., Mandarino, J.A., Maresch, W.V., Nickel, E.H., Rock, N.M.S., Schumacher, J.C., Smith, D.C., Stephenson, N.C.N., Ungaretti, L., Whittaker, L., and Youzhi, G. (1997) Nomenclature of amphiboles: Report of the subcommittee on amphiboles of the International Mineralogical Association, Commission on new minerals and minerals names. Canadian Mineralogist, 35, 219–246.

Litochleb, J., Novická, Z., and Burda, J. (1985) Vanadian garnets in Proterozoic metasilicites from Struhadlo near Klatovy. Časopis Národního Muzea Řada Přírodovědná, 151, 31–34 (in Czech).

Maheľ, M. (1986) Geological structure of Czechoslovak Carpathians, 1. Paleoalpine units, 510 p. Veda Press, Bratislava (in Slovak).

Maruyama, S., Suzuki, K., and Liou, J.G. (1983) Greenschist-amphibolite transition equilibria at low pressures. Journal of Petrology, 24, 583–604.

Moench, R.H. and Meyrowitz, R. (1964) Goldmanite, a vanadium garnet from Laguna, New Mexico. American Mineralogist, 49, 644–655.

Molák, B. and Slavkay, M. (1996) Role of black shales/schists in Variscan and Alpine metallogenic processes in the Western Carpathians. In P. Grecula and Z. Németh, Eds., Variscan metallogeny in the Alpine orogenic belt, p. 307–313. Mineralia Slovaca, Monography, Geocomplex Publishers, Bratislava.

Momoi, H. (1964) A new vanadium garnet, $(Mn,Ca)_3V_2Si_3O_{12}$, from the Yamato mine, Amami Islands, Japan. Memoires Faculty of Science Kyushu University, Series D, 15, 73–78.

Mueller, A.G. and Delor, C.P. (1991) Goldmanite-rich garnet in skarn veins, Southern Cross greenstone belt, Yilgarn Block, Western Australia. Mineralogical Magazine, 55, 617–620.

Novak, G.A. and Gibbs, G.V. (1971) The crystal chemistry of the silicate garnets. American Mineralogist, 56, 791–825.

Pan, Y. and Fleet, M.E. (1991) Vanadian allanite-(La) and vanadian allanite-(Ce) from the Hemlo gold deposit, Ontario, Canada. Mineralogical Magazine, 55, 497–507.

——— (1992) Mineral chemistry and geochemistry of vanadian silicates in the Hemlo gold deposit, Ontario, Canada. Contributions to Mineralogy and Petrology, 109, 511–525.

Plašienka, D., Korikovsky, S.P., and Hacura, A. (1993) Anchizonal Alpine metamorphism of Tatric cover sediments in the Malé Karpaty Mts., Western Carpathians. Geologica Carpathica, 44, 365–371.

Pouchou, J.-L. and Pichoir, F. (1985): "PAP" (phi-rho-z) procedure for improved quantitative microanalysis. In J.T. Armstrong, Ed., Microbeam analysis, p. 104–106. San Francisco Press, California.

Putiš, M. (1987) Geology and tectonics of southwestern and nothern part of the Malé Karpaty Mts. crystalline complex. Mineralia Slovaca, 19, 135–157 (in Slovak with English summary).

Putiš, M., Hrdlička, M., and Uher, P. (2004) Lithology and granitoid magmatism of Lower Palezoic in the Malé Karpaty Mts. Mineralia Slovaca, 36, 183–194 (in Slovak with English summary).

Sheldrick, G.M. (1997) SHELX-97. Program for the Solutions and Refinement of Crystal Structures. University of Göttingen, Germany.

Shepel, A.B. and Karpenko, M.V. (1969) Mukhinite, a new vanadium species of epidote. Doklady Akademii Nauk SSSR, Earth Sciences Section, 185, 1342–1345 (in Russian).

——— (1970) The first occurrence of goldmanite in SSSR. Doklady Akademii Nauk SSSR, Earth Sciences Section, 193, 906–908 (in Russian).

Shtukenberg, A.G., Popov, D.Yu., and Punin, Yu.O. (2002) An application of the point-dipole model to the problem of optical anomalies in grandite garnets. Mineralogical Magazine, 66, 275–286.

——— (2005) Growth ordering and anomalous birefringence in ugrandite garnets. Mineralogical Magazine, 69, 537–550.

Simon, S.B. and Grossman, L. (1992) Low-temperature exsolution in refractory siderophile element-rich opaque assemblages from the Leoville carbonaceous chondrite. Earth and Planetary Science Letters, 110, 67–75.

Slaughter, J., Kerrick, D.M., and Wall, V.J. (1975) Experimental and thermodynamic study of equilibria in the system CaO-MgO-SiO_2-H_2O-CO_2. American Journal of Science, 275, 143–162.

Strens, R.G.J. (1965) Synthesis and properties of calcium vanadium garnet (goldmanite). American Mineralogist, 50, 260.

Suwa, K., Suzuki, K., Miyakawa, K., and Agata, T. (1979) Vanadian and vanadium grossulars from the Mozambique metamorphic rocks, Mgama Ridge, Kenya. Preliminary Reports of African Studies, Nagoya University, 4, 87–96.

Takéuchi, Y., Haga, N., Umizu, S., and Sato, G. (1982) The derivative structure of silicate garnets in grandite. Zeitschrift für Kristallographie, 158, 53–99.

Uher, P., Chovan, M., and Majzlan, J. (1994) Vanadian-chromian garnet in mafic pyroclastic rocks of the Malé Karpaty Mts., Western Carpathians, Slovakia. Canadian Mineralogist, 32, 319–326.

von Knorring, O., Condliffe, E., and Tong, Y.L. (1986) Some mineralogical and geochemical aspects of chromium-bearing skarn minerals from northern Karelia, Finland. Bulletin of Geological Society of Finland, 58, 277–292.

Vrána, S. (1966) The veins with axinite and pumpellyite in the Malé Karpaty Mountains. Časopis pro mineralogii a geologii, 11, 415–421 (in Czech with English summary).

Wan, H.M. and Yeh, C.L. (1984) Uvarovite and grossular from the Fengtien nephrite deposits, eastern Taiwan. Mineralogical Magazine, 48, 31–37.

Wildner, M. and Andrut, M. (2001) The crystal chemistry of birefringent natural uvarovites: Part II. Single-crystal X-ray structures. American Mineralogist, 86, 1231–1251.

Manuscript received October 5, 2006
Manuscript accepted September 4, 2007
Manuscript handled by Daniel Harlov